Title

A glucocorticoid- and diet-responsive pathway toggles adipocyte precursor cell activity in vivo

Journal

Science Signaling, 9(451)

ISSN

1945-0877

Authors

Wong, Janica C
Krueger, Katherine C
Costa, Maria José
et al.

Publication Date

2016-10-25

DOI

10.1126/scisignal.aag0487

Peer reviewed

HHS Public Access

Author manuscript

Sci Signal. Author manuscript; available in PMC 2021 April 30.

Published in final edited form as:

Sci Signal. ; 9(451): ra103. doi:10.1126/scisignal.aag0487.

A glucocorticoid- and diet-responsive pathway toggles adipocyte precursor cell activity in vivo

Janica C. Wong[1], **Katherine C. Krueger**[1], **Maria José Costa**[1], **Abhishek Aggarwal**[1], **Hongqing Du**[1], **Tracey L. McLaughlin**[2], **Brian J. Feldman**[1,3,*]

[1]Department of Pediatrics/Endocrinology, Stanford University School of Medicine, Lokey Stem Cell Research Building, 259 Campus Drive, Stanford, CA 94305, USA.

[2]Department of Medicine/Endocrinology, Stanford University School of Medicine, 300 Pasteur Drive, Stanford, CA 94305, USA.

[3]Program in Regenerative Medicine, Stanford University School of Medicine, Lokey Stem Cell Research Building, Stanford, CA 94305, USA.

Abstract

Obesity is driven by excess caloric intake, which leads to the expansion of adipose tissue by hypertrophy and hyperplasia. Adipose tissue hyperplasia results from the differentiation of adipocyte precursor cells (APCs) that reside in adipose depots. Investigation into this process has elucidated a network of mostly transcription factors that drive APCs through the differentiation process. Using in vitro and in vivo approaches, our study revealed a signaling pathway that inhibited the initiation of the adipocyte differentiation program. Mouse adipocytes secreted the extracellular protease ADAMTS1, which triggered the production of the cytokine pleiotrophin (PTN) through the Wnt/β-catenin pathway, and promoted proliferation rather than differentiation of APCs. Glucocorticoid exposure in vitro or in vivo reduced ADAMTS1 abundance in adipocytes. In addition, mice fed a high-fat diet showed decreased *Adamts1* expression in the visceral perigonadal adipose depot, which expanded by adipogenesis in response to the diet, and increased *Adamts1* expression in the subcutaneous inguinal adipose depot, which did not induce adipogenesis. Similar to what occurred in mouse subcutaneous adipose tissue, diet-induced weight gain increased the expression of *ADAMTS1*, *PTN*, and certain Wnt target genes in the subcutaneous adipose depot of human volunteers, suggesting the relevance of this pathway to physiological adipose tissue homeostasis and the pathogenesis of obesity. Thus, this pathway

*Corresponding author. feldman@stanford.edu.

Author contributions: J.C.W. assisted in designing experiments, performed most of the experiments, and analyzed the data. K.C.K. assisted with the phenotyping of the *Adam Tg* mice and performed the microarray. M.J.C. performed and analyzed the microarray and assisted in verifying it. A.A. performed and analyzed the luciferase assays. H.D. generated the rADAM and assisted with the analysis of the adipogenesis experiments. T.L.M. conducted the overfeeding study and adipose tissue biopsies. B.J.F. designed experiments, analyzed results, and wrote the manuscript with input from all the authors.

Competing interests: Stanford University has filed a patent (PCT/US2013/070389) related to the discoveries described in this article.

Data and materials availability: The microarray data have been deposited into the Gene Expression Omnibus with accession no. GSE71427.

SUPPLEMENTARY MATERIALS

www.sciencesignaling.org/cgi/content/full/9/451/ra103/DC1

functions as a toggle on APCs, regulating a decision between differentiation and proliferation and coordinating the response of adipose tissue to systemic cues.

INTRODUCTION

Adipogenesis is the differentiation of adipocyte progenitor/stem cells into mature adipocytes and is a dynamic, highly controlled process (1–3). There is enormous interest in understanding the molecular regulation of adipogenesis with the anticipation that further insight will enable the development of novel therapeutic strategies to address the recalcitrant obesity problem along with the associated cardiovascular and metabolic diseases. Furthermore, once thought to be an inert energy storage depot, adipose tissue is actually a critical regulator of systemic homeostasis that secretes various hormones and other factors to influence diverse physiological processes (1, 4).

Insight into the process of adipogenesis has been advanced by studies using various cell lines, as well as the heterogeneous mixture of cells isolated from adipose tissue stroma [stromal vascular fraction (SVF)], that are readily induced to undergo differentiation in tissue culture using a cocktail of stimuli (5). This work has elucidated an elegant cell intrinsic network and a feedback system of primarily transcription factors that propels preadipocytes through the differentiation process (3, 6, 7). However, this experimental approach inherently bypasses the regulation of the induction of adipogenesis that occurs in vivo. The characterization of cell surface markers that permit identification, isolation, and tracing of a distinct population of adipocyte precursor cells (APCs) that are competent to reconstitute an adipose depot (8, 9) also enables probing of the regulation of adipogenesis in vivo.

In early life, substantial adipogenesis occurs to establish and expand the fat depots (10). Then, at a yet to be precisely defined time, the extent of adipogenesis decreases to plateau at a homeostatic levels with a turnover of around 10% of adipocytes per year with variability between depots (11, 12). Although the factors regulating the increase and subsequent postnatal decline in the rate of adipogenesis have not been identified, there is evidence that specific stimuli can reinduce an increase in the rate of adipogenesis above homeostatic levels. Introduction of a high-fat diet (HFD) is a factor that potently stimulates an increase in adipogenesis (13). Given the physiological nature of this stimulus and applicability to the current causes of the high rates of obesity, this process is particularly germane.

Glucocorticoids are an essential component of the cocktail used to induce differentiation in the in vitro differentiation of adipocyte progenitor cells (5). Glucocorticoids are a class of steroid hormones involved in the stress response and various other physiological processes that signal by binding to the glucocorticoid receptor to regulate the expression of target genes (14). Glucocorticoids—including dexamethasone, prednisone, and hydrocortisone—are commonly used medications because of their efficacy in treating various diseases including autoimmunity and cancer. However, patients who have excess circulating glucocorticoid concentrations frequently become obese (15).

Here, we identified ADAMTS1 as a glucocorticoid- and diet-responsive protein that potently inhibits APC activity in vivo. Our study revealed that ADAMTS1-mediated inhibition of APC differentiation occurred through an extracellular signaling pathway that translated systemic cues into a molecular switch to favor proliferation of APCs over differentiation. We showed that this control of APC activity involved a relay from *Adamts1* expression to Wnt signaling in APCs. Ingestion of HFD adipose depot specifically attenuated this pathway, thus allowing adipogenesis to proceed. Furthermore, we discovered that this pathway was conserved both in humans at the cellular level and in human volunteers in an overfeeding study.

RESULTS

Adamts1 abundance decreases in response to glucocorticoids

To identify glucocorticoid-responsive genes that might be involved in the in vivo regulation of adipogenesis, we analyzed microarrays performed with preadipocytes treated with the medically important synthetic glucocorticoid dexamethasone (16) and identified *Adamts1*. The expression of *Adam12* and *Adam23*, which are members of the related ADAM family and previously implicated to affect adipogenesis (17, 18), was not affected by dexamethasone in our expression profiling. ADAMTS1 is a member of the ADAMTS family of secreted proteins that affect morphogenesis, ovulation, arthritis, and cancer (19–21). We were particularly intrigued by ADAMTS1 because we reasoned that an extracellular protein might be well positioned to respond to systemic changes to modulate adipogenesis. To test this hypothesis, we analyzed adipose tissue from wild-type mice treated with dexamethasone and found that administration of systemic glucocorticoids caused a reduction in ADAMTS1 abundance in adipose tissue in vivo (Fig. 1A).

To begin to elucidate the role of *Adamts1* in adipose tissue, we fractionated the adipose depots from wild-type mice and compared *Adamts1* expression in purified mature adipocytes to that in the SVF. These studies indicate that mature adipocytes physiologically expressed significantly more *Adamts1* than the cells in the SVF (Fig. 1B). Furthermore, by performing both standard (fig. S1A) and ceiling culture assays (where mature adipocytes are cultured on the top internal surface of a well and secreted proteins condition the medium) (fig. S1B), we established that ADAMTS1 was secreted from wild-type mature adipocytes.

To study the function of *Adamts1* in adipose tissue in vivo, we generated transgenic mice in which *Adamts1* was overexpressed in the adipose tissue under the adipocyte *fatty acid binding protein 4* (*Fabp4*, also referred to as aP2) promoter and enhancer region (*Adam Tg*). We confirmed that ADAMTS1 was overexpressed in the adipose depots of *Adam Tg* mice (Fig. 1C), and excess ADAMTS1 was secreted from mature adipocytes purified from *Adam Tg* mice (fig. S1, A and B). Notably, we found that the adipose depots were significantly smaller in *Adam Tg* mice, although adipocyte size was modestly increased in these mice (Fig. 1, D and E). Total body weights and food intake were also similar in *Adam Tg* and wild-type littermates (fig. S1, C and D). The equivalent body weights suggest that the *Adam Tg* mice have altered body composition affecting other tissues.

ADAMTS1 inhibits adipogenesis and promotes the proliferation of APCs

We hypothesized that the decrease in adipose tissue mass in *Adam Tg* mice was caused by a block in adipogenesis generated by ADAMTS1-mediated signaling effects on APCs. To test this hypothesis, we injected 5-ethynyl-2′-deoxyuridine (EdU) into wild-type and *Adam Tg* mice. Because mature adipocytes do not divide, EdU-labeled (EdU^+) mature adipocytes must arise from the differentiation of dividing progenitor cells and therefore report the extent of adipogenesis that occurs during the chase period (22). Flow cytometry analysis of mature adipocytes purified from adipose tissues revealed that *Adam Tg* mice had significantly fewer EdU^+ mature adipocytes compared to wild-type littermates (Fig. 1F), suggesting that there was a block in the differentiation of APCs into adipocytes in these animals.

We further reasoned that a block in adipogenesis should result in the retention and thus expansion of the pool of undifferentiated APCs. Using flow cytometry with defined surface markers (8) to analyze endogenous APCs in vivo, we discovered that not only were there significantly more APCs in *Adam Tg* mice (Fig. 1G), there was also a substantial increase in the rate of proliferation of APCs in the *Adam Tg* mice compared to wild-type mice as quantified by measuring both Ki67 and EdU labeling of the APC population (Fig. 1, H and I, and fig. S2A). These results indicated that APCs in *Adam Tg* mice had an increased rate of proliferation in addition to the block in adipogenesis.

The *Fabp4* promoter/enhancers have low activity in APCs (23), and we confirmed that *Adamts1* was not overexpressed in APCs purified from *Adam Tg* mice compared to wild-type APCs (fig. S2B). These findings support the model that the APC phenotype of the *Adam Tg* mice resulted from an extracellular signal. To test this hypothesis, we exposed wild-type APCs to purified recombinant ADAMTS1 (rADAM) protein or bovine serum albumin (BSA) control protein while inducing adipocyte differentiation. The addition of rADAM substantially inhibited differentiation, as visualized under light microscopy (Fig. 2A) and by measuring the expression of genes encoding adipocyte differentiation markers (Fig. 2B). Inactivating the metalloproteinase activity in ADAMTS1 with an E402Q mutation diminished the block in differentiation (fig. S2, C and D). We also found that rADAM inhibited differentiation in 3T3-L1 preadipocytes (fig. S2E) (24), providing additional confirmation of the extracellular nature of the activity of ADAMTS1. Furthermore, rADAM increased the proliferation of both APCs and 3T3-L1 cells (Fig. 2C and fig. S2F). These studies indicated that both the block in differentiation and the increase in proliferation were caused by an extracellular ADAMTS1 signal targeting the APCs.

Induction of PTN is required for the effect of ADMATS1 on APCs

To identify the downstream pathway regulated by *Adamts1*, we compared the gene expression profiles of APCs isolated from wild-type and *Adam Tg* mice (fig. S3A). These unbiased studies identified *Ptn* (which encodes the cytokine pleiotrophin) as a gene with greatly increased expression in APCs from *Adam Tg* mice. Our expression profiling and confirmatory reverse transcription quantitative polymerase chain reaction (RT-qPCR) results revealed a ninefold increase in the expression of *Ptn* in APCs isolated from *Adam Tg* mice (fig. S3B). Verifying this result by another approach, we also found that exposing APCs isolated from wild-type mice to rADAM increased *Ptn* expression (Fig. 2D). In addition, we

found that *Ptn* expression (Fig. 2E) and PTN protein abundance (Fig. 2F) were substantially higher in the adipose tissue from *Adam Tg* compared to wild-type mice. Next, we injected wild-type mice with dexamethasone, which reduced PTN abundance in adipose tissue (Fig. 2G), suggesting that *Ptn* could be in the same pathway as *Adamts1* in regulating adipose tissue responsiveness to systemic glucocorticoids.

PTN is a member of the midkine family of heparin-binding growth factors with effects on development, immunity, and cancer (25, 26). PTN regulates stem and progenitor cell physiology and enhances the self-renewal and regeneration of hematopoietic stem cells (27, 28) and inhibits differentiation in 3T3-L1 cells (29, 30). When we analyzed the time course of adipocyte differentiation in APCs from wild-type mice, we discovered that endogenous *Ptn* abundance had a nadir between day 1 and day 3 after induction of adipocyte differentiation (fig. S3C), a critical time point when precursor cells commit to differentiate (31). The expression of *Ptn* in APCs isolated from *Adam Tg* mice remained higher (by a factor of >2) than that of wild-type APCs throughout the first 4 days of the adipocyte differentiation time course (fig. S3C). To examine whether extracellular PTN inhibited the differentiation of primary APCs, APCs isolated from wild-type mice were treated with recombinant PTN (rPTN) or BSA control protein while being induced to differentiate. These studies revealed that rPTN exposure inhibited differentiation in primary APCs and 3T3-L1 cells as visualized under light microscopy (Fig. 2H and fig. S3D) and quantified by measuring the expression of genes encoding adipocyte differentiation markers (Fig. 2I).

To test whether the induction of PTN was downstream of *Adamts1*, we used a neutralizing antibody against PTN (27) in vitro and in vivo. Coaddition of the PTN neutralizing antibody rescued the ADAMTS1-mediated block in adipocyte differentiation (Fig. 3, A and B), and injection of the neutralizing PTN antibody reversed the reduction in adipose tissue in the *Adam Tg* mice (Fig. 3, C and D). To confirm the mechanism of the rescue, we measured the relative numbers of EdU^+ APCs and mature adipocytes in wild-type and *Adam Tg* mice receiving control immunoglobulin G (IgG) or PTN antibody. We found that the in vivo administration of PTN neutralizing antibody rescued the *Adam Tg* phenotype by reducing the rate of APC proliferation and increasing adipogenesis to wild-type amounts (Fig. 3, E and F).

ADAMTS1 promotes Wnt signaling in APCs and enables cross-talk with glucocorticoid signaling

In neural cells, binding of PTN to the membrane receptor receptor protein tyrosine phosphatase β/ζ inhibits its intrinsic tyrosine phosphatase activity, resulting in increased tyrosine phosphorylation and nuclear translocation of β-catenin (32). In preadipocytes, β-catenin nuclear translocation and subsequent activation of T cell factor/lymphoid enhancer factor (TCF/LEF) transcription factors repress the transcription of *Pparγ*, which encodes a “master regulator” of adipogenesis (33–35). Therefore, we hypothesized that ADAMTS1 inhibited differentiation of APCs by activating the WNT/β-catenin signaling pathway, which we monitored through β-catenin localization. We discovered that the addition of rADAM to APCs from wild-type mice decreased the amount of β-catenin in the cytoplasmic fraction, while increasing it in the nuclear fraction (Fig. 4A), demonstrating an increase in the nuclear

translocation of β-catenin. Furthermore, treatment with rADAM increased the expression of TCF/LEF target genes in APCs (Fig. 4B). In addition, we found that FACS-purified APCs directly harvested from *Adam Tg* mice had increased expression of TCF/LEF target genes compared to those from wild-type mice (Fig. 4C), establishing that Adamts1 was connected to Wnt signaling in vivo. Moreover, we discovered that in vivo neutralization of PTN restored endogenous Wnt signaling in APCs from *Adam Tg* mice to wild-type amounts (Fig. 4D), and administration of the small-molecule Wnt inhibitor IWP2 (36) partially rescued APCs from the ADAMTS1-mediated block in adipogenesis (Fig. 4, E and F). These results indicated that ADAMTS1 stimulation of the PTN-Wnt pathway was critical for its activity on APCs. We also discovered that administration of systemic dexamethasone to wild-type mice decreased *Axin2* expression in APCs, and this effect was blocked in *Adam Tg* mice (Fig. 4G). These findings revealed that the glucocorticoid-responsive Adamts1 pathway was a mechanism for decreasing Wnt signaling in vivo to alter the activity of APCs.

ADAMTS1 induces *Ptn* expression by a feed-forward Wnt signal

Expression profiling (fig. S3) and cell autonomous experiments with rADAM (Fig. 2D) revealed that ADAMTS1 increased *Ptn* expression. However, we wondered how this process was mediated because ADAMTS1 is an extracellular protein. We hypothesized that the induction of *Ptn* expression by ADAMTS1 resulted from stimulation of Wnt signaling because ADAMTS1 caused nuclear translocation of β-catenin (Fig.4A), and β-catenin regulated the expression of target genes through its interactions with TCF/LEF. Inhibiting Wnt signaling with IWP2 was sufficient to block the induction of *Ptn* expression by ADAMTS1 (Fig. 4H), confirming our hypothesis. In addition, we tested whether *Ptn* was a direct TCF/LEF target gene and whether ADAMTS1 induction of *Ptn* expression occurred by the stimulation of Wnt signaling promoting the activity of TCF/LEF on the *Ptn* gene. First, we identified a putative TCF/LEF binding site located ~1 kb upstream of the transcriptional start site (TSS) in the promoter-proximal region of the *Ptn* gene. Next, we performed luciferase reporter assays using a construct with the endogenous *Ptn* promoter and promoter-proximal region containing the putative TCF/LEF binding site. We found that exposing cells transfected with this reporter construct to rADAM induced promoter activity, and this induction of *Ptn* promoter activity by rADAM was blocked by IWP2 (Fig. 4I).

HFD induces differential responses in the ADAMTS1-PTN-Wnt pathway in an adipose depot–specific manner

We were interested to test whether the ADAMTS1-PTN-Wnt pathway was responsive to physiological stimuli that control the rate of adipogenesis. Consistent with other work (11, 37), monitoring of adipose depots in humans using ^{14}C labeling from exposure to nuclear bomb testing by Spalding *et al.* (12) reveals that obese individuals have significantly more adipocytes added per year compared to lean individuals. Diet-induced obesity in mice fed an HFD models this human response of increased adipogenesis (13, 22). This response to HFD is depot-specific, with the increase in adipogenesis mostly restricted to visceral depots, although the subcutaneous depots expand by hypertrophy and have minimal change in the amount of adipogenesis (13). We speculated that the ADAMTS1 signal would be relevant to connecting an HFD to the induction of adipogenesis in APCs. Therefore, we fed a HFD to wild-type mice to increase the sizes of the visceral gWAT and subcutaneous iWAT fat depots

(Fig. 5A). Using EdU chase experiments, we confirmed that HFD induced adipogenesis in wild-type mice in the gWAT depot but not in the iWAT depot (Fig. 5B), as has been previously reported (13). Furthermore, the HFD resulted in a corresponding depot-specific response in the expression of *Adamts1* and *Ptn*. In the iWAT depot, expression of both *Adamts1* and *Ptn* increased, whereas in the gWAT depot, expression of these genes significantly decreased (Fig. 5C). Furthermore, we found that the HFD induced corresponding depot-specific changes in Wnt target gene expression in APCs from iWAT compared to gWAT depots (Fig. 5D).

Because *Adamts1* expression was responsive to glucocorticoids, we wondered whether the changes in response to HFD were altered by depot-specific differences in physiological glucocorticoids. The 11β-hydroxysteroid dehydrogenase type 1 and 2 enzymes (11βHSD1 and 11βHSD2) tissue-specifically control endogenous glucocorticoids by regulating the local interconversions between the inactive and active forms of the hormone (38). Therefore, we tested whether there was adipose depot–specific regulation of the expression of these enzymes in response to HFD. Remarkably, we discovered that HFD induced *Hsd11b1* expression (the enzyme encoded by this gene activates endogenous glucocorticoids) specifically in the gWAT depot, whereas expression of *Hsd11b2* (the enzyme encoded by this gene inactivates glucocorticoids) was induced in the iWAT (Fig. 5E). These data support a model in which ingestion of HFD results in depot-specific changes in endogenous glucocorticoid signaling, which alters the amount of ADAMTS1 signaling to coordinate the depot-specific induction of adipogenesis. To test whether the reduction in *Adamts1* expression in the gWAT in response to HFD was essential for permitting the induction of adipogenesis in this tissue, we examined whether the *Adam Tg* mice (which constitutively express *Adamts1* in adipose tissue, and therefore, ADAMTS1 abundance in the adipose tissue bypasses regulation by the 11βHSD enzymes) were resistant to HFD-induced adipogenesis in the gWAT. We discovered that the induction of adipogenesis in the gWAT with 3 months of HFD feeding was blocked in the *Adam Tg* mice (Fig. 5F). Together, these data indicate that HFD feeding reduced Adamts1 signaling in gWAT, which released the differentiation block on APCs.

The ADAMTS1-PTN-Wnt pathway is conserved in human adipose cells

We next tested for evidence that this pathway was present and functionally conserved in humans. As observed in mice, we found that overexpression of *ADAMTS1* in human adipose tissue SVF obtained from healthy donors induced the expression of *PTN* (Fig. 6A) and TCF/LEF target genes (Fig. 6B). Furthermore, we found that human rADAM and rPTN inhibited adipocyte differentiation of human SVF, similar to our results in mouse cells (Fig. 6, C and D). We also found that neutralizing PTN both rescued the ADAMTS1-mediated block in adipocyte differentiation (Fig. 6, C and D) and blunted the induction of the expression of TCF/LEF target genes (Fig. 6E), demonstrating pathway conservation at the functional level in human cells. In addition, we discovered that human rADAM and rPTN increased the rate of proliferation of human SVF cells and the Simpson-Golabi-Behmel syndrome (SGBS) human preadipocyte cell line (39) (fig. S4, A to C), analogous to what we observed with mouse cells.

The ADAMTS1-PTN-Wnt pathway responds to overfeeding in humans

The in vitro studies with human cells validated that the Adamts1 pathway that we identified was conserved in humans. We next sought to ascertain that this pathway was also relevant in vivo in humans with adipose tissue samples from a trial of overfeeding-induced weight gain in humans. In this trial, subcutaneous adipose tissue biopsies from female volunteers with body mass indexes (BMIs) of 25 to 35 kg/m^2 were obtained (obtaining visceral adipose tissue samples in these healthy volunteers was not feasible). The participants were then started on a 4-week course of caloric overfeeding that was supervised by a dietitian and resulted in an average weight gain of 3.5 kg. At the end of the 4 weeks of overfeeding, subcutaneous adipose tissue samples were taken from the volunteers. HFD increased the expression of *Adamts1* and *Ptn* in the subcutaneous adipose tissue of mice (Fig. 5C), and similarly, we found that overfeeding induced both *ADAMTS1* and *PTN* expression in the subcutaneous adipose tissue of healthy humans (Fig. 6F). Finally, we discovered that the expression of TCF/LEF target genes was also increased in the subcutaneous SVF of the volunteers after overfeeding (Fig. 6G), suggesting that Wnt signaling was altered in response to the hypercaloric diet, as occurred in the HFD mouse model (Fig. 5E). These data suggested that the response of the ADAMTS1 pathway to changes in diet was conserved in humans.

DISCUSSION

Although reductionist studies in tissue culture have revealed molecular details about the process of adipogenesis, there is less information about the factors that gate the initiation of this differentiation cascade, particularly in vivo. The results of this study demonstrated that *Adamts1* connected systemic glucocorticoids or the ingestion of an HFD to APC activity. Our studies elucidated that the response of adipose tissue to these systemic factors was coordinated by changes in *Adamts1* and *Ptn* expression, switching on Wnt signaling in APCs. Notably, these signaling pathways from glucocorticoids and HFD also identified previously unrecognized modes for in vivo activation of WNT/β-catenin in APCs.

These findings provide insight into how adipose tissue responds to changes in the systemic environment. Changes in dietary intake can have a major impact on adipose tissue (40, 41). Intuitively, a HFD leads to increased adipose depot mass, and high-calorie diets are broadly recognized as a leading cause of the rise in obesity over the past several decades (42). Therefore, elucidating the pathways by which a high-calorie diet generates a cellular signal governing adipogenesis might lead to the development of new approaches for the treatment and prevention of obesity. Furthermore, increasing evidence suggests that, at least for some individuals, the progression from obesity to the development of insulin resistance and diabetes includes perturbations to the physiological regulation of adipogenesis (43). Therefore, exposing the pathways that regulate adipogenesis in vivo could be a critical step to developing strategies that can intercept this process. It will be interesting to evaluate whether alterations to the pathway identified in this study are relevant for the pathogenesis of type 2 diabetes.

The extracellular nature of the pathway that we revealed is intriguing, if not surprising, because a simpler and more direct input into APCs could be envisioned. It is tempting to

speculate that this system evolved as a means for adipose tissue to communicate with APCs to respond to changing needs and systemic signals. It is also possible that the extracellular environment uniquely enables combining of the ADAMTS1 signal with competing and synergizing endocrine, paracrine, and other systemic inputs that are integrated by the APC to determine activity. Previous studies on fibroblast growth factor 21 (FGF21) are also consistent with this model: Although, to our knowledge, FGF21 effects on endogenous APC proliferation or differentiation have not yet been reported, systemic administration of peroxisome proliferator–activated receptor γ (PPARγ) agonists induces *Fgf21* expression in adipose tissue (44). Jonker *et al.* (45) have demonstrated that recombinant FGF21 added to the medium of stromal vascular cells in culture promotes adipogenesis by modulating PPARγ activity. Collectively with our results, a new model emerges from these findings in which changes in the systemic environment are integrated by adipocytes, which then relay regulatory signals to the local precursor cell population to instruct the adipose tissue response.

In conclusion, we identified an ADAMTS1-PTN-Wnt pathway that converts systemic changes into a cellular signal in adipose tissue. We found that this signaling pathway controlled the physiologically important decision for APCs to proliferate or differentiate in vivo. Uncovering that this pathway responds to glucocorticoids provides a new understanding of how the initiation of adipogenesis is gated in vivo and offers insights into the effects of systemic glucocorticoids on adipose tissue. Moreover, we discovered that this pathway was also responsive to the physiological stimulus of HFD in wild-type mice and is conserved in humans. In summary, these findings reveal a previously unrecognized control mechanism for adipose tissue to respond to systemic cues, including increased caloric intake, by adjusting the rate of adipogenesis.

MATERIALS AND METHODS

Mice

All studies were approved by Stanford University's Administrative Panel on Laboratory Animal Care Committee. The full coding sequence of the *Adamts1* complementary DNA (cDNA) was generated by RT-PCR of RNA isolated from differentiated mouse adipocytes. The *Adamts1* transgene was generated by subcloning the complete coding sequence of *Adamts1* downstream of a 7.6 *Fabp4* promoter/enhancer fragment and in front of a poly(A) sequence (gift from O. MacDougald, University of Michigan). The purified transgene was microinjected into friend virus B (FVB) pronuclei of fertilized oocytes, and the oocytes were transplanted into pseudopregnant mice. Three founder lines were generated that all had a similar phenotype. The data presented are derived from the line with the lowest amount of overexpression of *Adamts1* in the adipose tissue. Gender-matched littermates were used as controls. For the HFD experiments in wild-type mice, 10-week-old male C57BL/6J mice were purchased from Jackson Laboratories and fed a diet with 60% kilocalories from fat (Bio-Serv, F3282) ad libitum for 3 months.

Human samples

Human SVF (Zen-Bio) isolated from lean subjects (BMI, <24.99) were used for in vitro adipogenesis and XTT assays. Adipogenesis was induced as described below. Adipose tissue samples from healthy (nondiabetic) volunteers before and after overfeeding were obtained after informed consent in accordance with protocols approved by the Stanford Institutional Review Board. Adipose tissue samples were obtained by periumbilical scalpel biopsy of the subcutaneous fat at the time of enrollment (baseline). Volunteers then began weight gain intervention by overfeeding, which was supervised by weekly visits to a dietitian at Stanford Hospital. After 4 weeks of weight gain, repeat adipose tissue samples were obtained. Patients had an average weight gain of 3.5 kg.

FACS of APCs

Animals were euthanized by asphyxiation with CO_2 and cervical dislocation, and adipose depots were dissected. The adipose tissues were minced and incubated in collagenase (1 mg/ml) (Worthington) in Dulbecco's modified Eagle's medium (DMEM)/F12 for 1 hour at 37°C with 5% CO_2. After inactivation of the digestion with an equal volume of DMEM/10% fetal bovine serum (FBS), samples were passed through 100-μm cell strainers. After inactivation with Hanks' balanced salt solution (HBSS)/2% FBS, samples were centrifuged and resuspended in 1 ml of ACK Lysing Buffer (Lonza) to remove red blood cells. Cells were pelleted again and resuspended in HBSS/2% FBS for antibody labeling for flow cytometry or FACS. The following antibodies were used: SCA1 fluorescein isothiocyanate (FITC) (BD, 557405), CD45 phycoerythrin (PE)–Cy7 (eBioscience, 25-0421-82), and CD31 APC (eBioscience, 17-0311-82). Samples were analyzed on a BD FACSAria II in the Stanford Stem Cell Institute FACS core. Cell gating was based on comparison with unstained and fluorescence minus one–stained controls. Single live cells were discriminated by forward-scatter and side-scatter analyses and 7-aminoactinomycin D (7-AAD) labeling (BD Biosciences). Cells were sorted into serum-free DMEM for gene expression analysis or into complete medium for cell culture. Flow cytometry standard files were analyzed using FlowJo version 10.

In vivo EdU labeling

EdU (Carbosynth) was administered by intraperitoneal injections (100 mg/kg) once every day for 2 weeks. For flow cytometric analysis, SVF was prepared and stained for surface markers as previously described using the following antibodies: SCA1 APC (BioLegend, 108112), CD45 PE-Cy7 (eBioscience, 25-0421-82), and CD31 PE-Cy7 (eBioscience, 25-0311-81). Samples were then fixed in 4% paraformaldehyde (PFA)/phosphate-buffered saline (PBS) for 30 min and then permeabilized in 1× saponin-based permeabilization buffer (Invitrogen) for 10 min. EdU was labeled using the Click-iT EdU Alexa Fluor 488 Flow Cytometry Assay Kit (Invitrogen) by following the manufacturer's protocol. For adipocyte EdU-labeled nuclei analysis, adipocyte nuclei were isolated in cold nuclei extraction buffer [320 mM sucrose, 5 mM $MgCl_2$, 10 mM Hepes, and 2% Triton X-100 (pH 7.4)] in a Dounce homogenizer. Nuclei were centrifuged at 3000*g* for 15 min and washed with cold nuclei wash buffer [320 mM sucrose, 5 mM $MgCl_2$, 10 mM Hepes, 1% BSA, and 0.1% sodium azide (pH 7.4)]. EdU nuclei were labeled using the Click-iT EdU Alexa Fluor 488 Flow

Cytometry Assay Kit. DAPI (4′,6-diamidino-2-phenylindole) (500 ng/ml) was added to cells or nuclei immediately before FACS analysis. EdU gating was based on samples isolated from mice with no EdU injection (fig. S2).

Cell culture

Primary SVF and APCs were maintained in DMEM with 10% FBS (Atlanta Biologicals), streptomycin (50 μg/ml), and penicillin (50 units/ml) (Lonza). 3T3-L1 cells were maintained in DMEM with 10% fetal calf serum (FCS), streptomycin (50 μg/ml), and penicillin (50 units/ml) (Life Technologies). The SGBS cell line was maintained in DMEM/F12 supplemented with pantothenate (4×10^{-3} mg/ml), biotin (8×10^{-3} mg/ml), streptomycin (50 μg/ml), and penicillin (50 units/ml). Cells were cultured at 37°C in an atmosphere of 5% CO_2/95% air.

For the ceiling cultures, mature adipocytes were isolated from adipose tissue by collagenase digestion and washed with PBS. The washed adipocytes were plated into collagen-coated (1 mg/ml) flasks filled to the ceiling with DMEM and 20% FCS as previously described (46). Adipocytes were allowed to adhere to the ceiling of the flask for 10 days. The attached adipocytes were then incubated in reduced serum culture medium [DMEM with 2% FBS and insulin (1 μg/ml)] for 48 hours.

Scanning electron microscopy

Tissue samples were fixed in 4% PFA with 2% glutaraldehyde in 0.1 M sodium cacodylate buffer (pH 7.4) for 24 to 48 hours at 4°C, rinsed in the same buffer, and postfixed in 1% aqueous OsO_4 for 2 hours before dehydration in an increasing ethanol series (50-70-90-100%, 15 min each). Samples were freeze-fractured in liquid nitrogen using a Leica EMCPC (Leica Microsystems), followed by hexamethyldisilazane drying. All samples were subsequently mounted on aluminum pin stubs and visualized with a Hitachi 3400N scanning electron microscope (SEM) using secondary electron detection at 5 to 15 kV.

Microarray analysis

APCs were isolated by FACS from the iWAT of *Adam1 Tg* mice and littermate wild-type controls at 5 weeks of age. Total RNA from the APCs was isolated using RNeasy Micro Kit (Qiagen). Total RNA was processed using the Agilent Low Input Quick Amp single-color labeling kit and hybridized on a SurePrint G3 8×60K mouse array (Agilent). Microarray data were analyzed with GeneSpring GX v11 software.

Adenovirus infection

Human SVF cells were grown to 80% confluency in 24-well plates. Cells were incubated in growth medium with ADAMTS1-encoding adenovirus(Cyagen)according to the manufacturer’s protocol. Ad-GFP was used as the control. Cells were harvested 24 hours after infection for RT-qPCR.

Cell fractionation

Nuclear and cytoplasmic protein extraction was performed using the NE-PER Nuclear and Cytoplasmic Extraction kit (Thermo Scientific, PI-78833) following the manufacturer's protocol.

Immunoblots

Cells were lysed using 85°C SDS lysis buffer [50 mM tris-HCl (pH 6.8), 2% SDS, 10 mM dithiolthreitol, and 10% glycerol]. Total protein was measured by Bradford analysis. The proteins were resolved by electrophoresis in 10% SDS polyacrylamide gels and transferred to polyvinylidene difluoride membranes. Membranes were blocked at room temperature for 1 hour with blocking buffer (LI-COR Biosciences) with 0.05% Tween, followed by overnight incubation with the primary antibody [ADAMTS1 (1:1000) (R&D Systems), PTN (1:1000) (R&D Systems), β-catenin (1:1000) (GenScript), Lamin A/C (1:2000) (Cell Signaling Technology), β-tubulin (1:2000) (GenScript), or β-actin (1:2000) (GenScript)] and subsequently with secondary antibodies labeled with infrared dyes (LI-COR Biosciences) (1:25,000 in blocking buffer; room temperature for 1 hour). The membranes were scanned on the Odyssey infrared imaging system (LI-COR Biosciences).

In vitro recombinant protein and PTN neutralizing antibody assays

rADAM and rPTN (R&D, 5867-AD-020 and 252-PL-050) were coated overnight at 4°C on 3-μm polystyrene latex beads (Sigma, LB30–2ML). rADAM, rPTN, and PTN neutralizing antibody (R&D, AF-252-PB; 2.5 μg/ml) were added every other day in adipogenesis assay. For the adipogenesis experiments comparing the effects wild-type and E402Q ADAMTS1, full-length *Adamts1* cDNA was subcloned into a pEF6 expression vector (Invitrogen) in-frame with His and V5 tags. PCR-based site-directed mutagenesis was used to create the mutation in *Adamts1* and was confirmed by sequencing. Clonal stable Chinese hamster ovary cell lines expressing wild-type or E402Q ADAMTS1 were established by transfecting cells with the expression vectors (Lipofectamine 2000, Invitrogen), followed by selection with blasticidin (5 μg/ml) and single-cell isolation by limiting dilution. The cell culture supernatants of the ADAMTS1 and E402Q ADAMTS1 cell lines were collected and purified through Ni-NTA Agarose (MCLAB). The purified proteins were analyzed on polyacrylamide gels and by Western blot.

Luciferase assays

A plasmid containing the human *Ptn* promoter and proximal region (~1 kb upstream from TSS) (SwitchGear Genomics) was transfected into human embryonic kidney–293T cells using Lipofectamine 2000 (Life Technologies) according to the manufacturer's protocol. Cells were treated with rADAM (800 ng/ml) and IWP2 (2 μM/ml). Luciferase assays were performed using a Luciferase Assay System (SwitchGear Genomics) according to the manufacturer's instructions, and luminescence was quantified using a plate reader (BioTek).

In vivo dexamethasone treatment

Dexamethasone 21-phosphate (Sigma, D1159), dissolved in PBS, was administered by intraperitoneal injection (10 mg/kg) into 5-week-old male mice once every other day for 10 days.

In vivo PTN neutralization antibody injections

PTN neutralizing antibody (R&D, AF-252-PB) was administered by intraperitoneal injection (50 μg/kg) once every other day for 2 weeks. Injections of normal goat IgG (R&D, AB-108-C) at 50 μg/kg were used as controls.

Ki67 measurement

SVF was prepared as previously described. Samples were then fixed in 4% PFA/PBS for 30 min and permeabilized in 1× permeabilization buffer (BD Biosciences) for 10 min. APC cell surface markers were stained as previously described with the following exception. Cells were stained with the following antibodies: SCA1 FITC (BD, 557405), CD45 APC (BioLegend, 103112), CD31 APC (eBioscience, 17-0311-82), Ki67 PE-Cy7 (eBioscience, 25-5698-80), and DAPI. Samples were then analyzed on a BD FACSAria II. Ki67 gating was based on comparison with unstained and fluorescence minus Ki67–stained controls.

XTT assays

Cells were seeded in 96-well plates in 100 μl of DMEM for 24 hours. XTT (MP Biomedicals) solution was prepared fresh at 1 mg/ml in phenazine methosulfate (0.6 mg/ml)/PBS solution. Equal volume of XTT solution (100 μl) was added to each well for 3 hours at 37°C. The amount of water-soluble product generated from XTT is proportional to the number of living cells in the sample and was quantified by measuring absorbance at a wavelength of 450 nm using a BioTek Synergy H1 plate reader.

Reverse transcription quantitative polymerase chain reaction

Total RNA was extracted using the Hybrid-R kit (GeneAll) according to the manufacturer's protocol. Equal amounts of RNA were reverse-transcribed (200 ng of RNA for a 20-μl reverse transcription reaction) using random priming, and relative transcript amounts were measured by qPCR using a CFX384 system (Bio-Rad). Primer sequences are listed in table S1.

Adipocyte differentiation assays

APCs were seeded into 96-well plates (Falcon) and allowed to grow to confluence. Cells were maintained at confluence for 2 days and then induced with the differentiation cocktail [1 μM dexamethasone, insulin (1 μg/ml), and 0.5 mM 3-isobutyl-1-methylxanthine] for 2 days. Thereafter, cells were maintained in maintenance medium [culture medium with insulin (1 μg/ml)], which was changed every other day. Differentiation was allowed to continue for a total of 8 days. Cells were photographed under a phase microscope (Nikon).

Statistical analysis

Statistical analysis was performed by one- or two-way analysis of variance (ANOVA) using GraphPad Prism software. Differences between experimental groups were determined by *t* test or Dunnett's post hoc test.

Supplementary Material

Refer to Web version on PubMed Central for supplementary material.

Acknowledgments:

We thank members of the Feldman laboratory for helpful discussions. We thank R. Nusse (Stanford University) for the IWP2 compound. We thank L.-M. Joubert (Stanford University) and the Stanford Microscopy Facility for technical assistance with the SEM.

Funding:

The work was funded by an NIH Director's New Innovator Award (DP2 OD006740) and the Stanford SPARK Translational Research Program at Stanford and the Glenn Foundation for Medical Research to B.J.F. Support for K.C.K. and J.C.W. was provided by NIH (grant T32 DK007217). K.C.K. and M.J.C. were supported by the Stanford School of Medicine Dean's Postdoctoral Fellowship. J.C.W., K.C.K., M.J.C., A.A., and H.D. were supported by the Lucile Packard Foundation for Children's Health, Stanford NIH–National Center for Advancing Translational Sciences–Clinical and Translational Science Awards (UL1 TR001085), and Child Health Research Institute of Stanford University. T.L.M. was supported by a grant from the American Diabetes Association (1-11-CT-35). B.J.F. is the Bechtel Endowed Faculty Scholar in Pediatric Translational Medicine.

REFERENCES AND NOTES

1. Berry DC, Stenesen D, Zeve D, Graff JM, The developmental origins of adipose tissue. Development 140, 3939–3949 (2013). [PubMed: 24046315]
2. Rosen ED, MacDougald OA, Adipocyte differentiation from the inside out. Nat. Rev. Mol. Cell Biol 7, 885–896 (2006). [PubMed: 17139329]
3. Cristancho AG, Lazar MA, Forming functional fat: A growing understanding of adipocyte differentiation. Nat. Rev. Mol. Cell Biol 12, 722–734 (2011). [PubMed: 21952300]
4. Rosen ED, Spiegelman BM, What we talk about when we talk about fat. Cell 156, 20–44 (2014). [PubMed: 24439368]
5. MacDougald OA, Mandrup S, Adipogenesis: Forces that tip the scales. Trends Endocrinol. Metab 13, 5–11 (2002). [PubMed: 11750856]
6. Farmer SR Transcriptional control of adipocyte formation. Cell Metab. 4, 263–273 (2006). [PubMed: 17011499]
7. Lefterova MI, Haakonsson AK, Lazar MA, Mandrup S, Pparγ and the global map of adipogenesis and beyond. Trends Endocrinol. Metab 25, 293–302 (2014). [PubMed: 24793638]
8. Rodeheffer MS, Birsoy K, Friedman JM, Identification of white adipocyte progenitor cells in vivo. Cell 135, 240–249 (2008). [PubMed: 18835024]
9. Tang W, Zeve D, Suh JM, Bosnakovski D, Kyba M, Hammer RE, Tallquist MD, Graff JM, White fat progenitor cells reside in the adipose vasculature. Science 322, 583–586 (2008). [PubMed: 18801968]
10. Kirtland J, Harris PM, Changes in adipose tissue of the rat due to early undernutrition followed by rehabilitation. 3. Changes in cell replication studied with tritiated thymidine. Br. J. Nutr 43, 33–43 (1980). [PubMed: 7370216]
11. Prins JB, O'Rahilly S, Regulation of adipose cell number in man. Clin. Sci. (Lond.) 92, 3–11 (1997). [PubMed: 9038586]

12. Spalding KL, Arner E, Westermark PO, Bernard S, Buchholz BA, Bergmann O, Blomqvist L, Hoffstedt J, Näslund E, Britton T, Concha H, Hassan M, Rydén M, Frisén J, Arner P, Dynamics of fat cell turnover in humans. Nature 453, 783–787 (2008). [PubMed: 18454136]
13. Wang QA, Tao C, Gupta RK, Scherer PE, Tracking adipogenesis during white adipose tissue development, expansion and regeneration. Nat. Med 19, 1338–1344 (2013). [PubMed: 23995282]
14. Miranda TB, Morris SA, Hager GL, Complex genomic interactions in the dynamic regulation of transcription by the glucocorticoid receptor. Mol. Cell. Endocrinol 380, 16–24 (2013). [PubMed: 23499945]
15. Johannsson G, Ragnarsson O, Cardiovascular and metabolic impact of glucocorticoid replacement therapy. Front. Horm. Res 43, 33–44 (2014). [PubMed: 24943296]
16. So AY-L, Cooper SB, Feldman BJ, Manuchehri M, Yamamoto KR, Conservation analysis predicts in vivo occupancy of glucocorticoid receptor-binding sequences at glucocorticoid-induced genes. Proc. Natl. Acad. Sci. U.S.A 105, 5745–5749 (2008). [PubMed: 18408151]
17. Kurisaki T, Masuda A, Sudo K, Sakagami J, Higashiyama S, Matsuda Y, Nagabukuro A, Tsuji A, Nabeshima Y, Asano M, Iwakura Y, Sehara-Fujisawa A, Phenotypic analysis of meltrin α (ADAM12)-deficient mice: Involvement of meltrin α in adipogenesis and myogenesis. Mol. Cell. Biol 23, 55–61 (2003). [PubMed: 12482960]
18. Kim HA, Park W-J, Jeong H-S, Lee H.-e., Lee SH, Kwon NS, Baek KJ, Kim D-S, Yun H-Y, Leucine-rich glioma inactivated 3 regulates adipogenesis through ADAM23. Biochim. Biophys. Acta 1821, 914–922 (2012). [PubMed: 22405860]
19. Apte SS, A disintegrin-like and metalloprotease (reprolysin-type) with thrombospondin type 1 motif (ADAMTS) superfamily: Functions and mechanisms. J. Biol. Chem 284, 31493–31497 (2009). [PubMed: 19734141]
20. Tan Ide A, Ricciardelli C, Russell DL, The metalloproteinase ADAMTS1: A comprehensive review of its role in tumorigenic and metastatic pathways. Int. J. Cancer 133, 2263–2276 (2013). [PubMed: 23444028]
21. Tang BL, ADAMTS: A novel family of extracellular matrix proteases. Int. J. Biochem. Cell Biol 33, 33–44 (2001). [PubMed: 11167130]
22. Jeffery E, Church CD, Holtrup B, Colman L, Rodeheffer MS, Rapid depot-specific activation of adipocyte precursor cells at the onset of obesity. Nat. Cell Biol 17, 376–385 (2015). [PubMed: 25730471]
23. Krueger KC, Costa MJ, Du H, Feldman BJ, Characterization of cre recombinase activity for in vivo targeting of adipocyte precursor cells. Stem Cell Rep. 3, 1147–1158 (2014).
24. Green H, Kehinde O, An established preadipose cell line and its differentiation in culture. II. Factors affecting the adipose conversion. Cell 5, 19–27 (1975). [PubMed: 165899]
25. Kadomatsu K, Kishida S, Tsubota S, The heparin-binding growth factor midkine: The biological activities and candidate receptors. J. Biochem 153, 511–521 (2013). [PubMed: 23625998]
26. Deuel TF, Zhang N, Yeh H-J, Silos-Santiago I, Wang Z-Y, Pleiotrophin: A cytokine with diverse functions and a novel signaling pathway. Arch. Biochem. Biophys 397, 162–171 (2002). [PubMed: 11795867]
27. Himburg HA, Harris JR, Ito T, Daher P, Russell JL, Quarmyne M, Doan PL, Helms K, Nakamura M, Fixsen E, Herradon G, Reya T, Chao NJ, Harroch S, Chute JP, Pleiotrophin regulates the retention and self-renewal of hematopoietic stem cells in the bone marrow vascular niche. Cell Rep. 2, 964–975 (2012). [PubMed: 23084748]
28. Himburg HA, Yan X, Doan PL, Quarmyne M, Micewicz E, McBride W, Chao NJ, Slamon DJ, Chute JP, Pleiotrophin mediates hematopoietic regeneration via activation of RAS. J. Clin. Invest 124, 4753–4758 (2014). [PubMed: 25250571]
29. Gu D, Yu B, Zhao C, Ye W, Lv Q, Hua Z, Ma J, Zhang Y, The effect of pleiotrophin signaling on adipogenesis. FEBS Lett. 581, 382–388 (2007). [PubMed: 17239862]
30. Yi C, Xie W.-d., Li F, Lv Q, He J, Wu J, Gu D, Xu N, Zhang Y, MiR-143 enhances adipogenic differentiation of 3t3-L1 cells through targeting the coding region of mouse pleiotrophin. FEBS Lett. 585, 3303–3309 (2011). [PubMed: 21945314]

31. Ahrends R, Ota A, Kovary KM, Kudo T, Park BO, Teruel MN, Controlling low rates of cell differentiation through noise and ultrahigh feedback. Science 344, 1384–1389 (2014). [PubMed: 24948735]
32. Meng K, Rodriguez-Pena A, Dimitrov T, Chen W, Yamin M, Noda M, Deuel TF, Pleiotrophin signals increased tyrosine phosphorylation of beta β-catenin through inactivation of the intrinsic catalytic activity of the receptor-type protein tyrosine phosphatase β/ζ. Proc. Natl. Acad. Sci. U.S.A 97, 2603–2608 (2000). [PubMed: 10706604]
33. Prestwich TC, Macdougald OA, Wnt/β-catenin signaling in adipogenesis and metabolism. Curr. Opin. Cell Biol 19, 612–617 (2007). [PubMed: 17997088]
34. Park KW, Halperin DS, Tontonoz P, Before they were fat: Adipocyte progenitors. Cell Metab. 8, 454–457 (2008). [PubMed: 19041761]
35. Zeve D, Seo J, Suh JM, Stenesen D, Tang W, Berglund ED, Wan Y, Williams LJ, Lim A, Martinez MJ, McKay RM, Millay DP, Olson EN, Graff JM, Wnt signaling activation in adipose progenitors promotes insulin-independent muscle glucose uptake. Cell Metab. 15, 492–504 (2012). [PubMed: 22482731]
36. Chen B, Dodge ME, Tang W, Lu J, Ma Z, Fan C-W, Wei S, Hao W, Kilgore J, Williams NS, Roth MG, Amatruda JF, Chen C, Lum L, Small molecule–Mediated disruption of Wnt-dependent signaling in tissue regeneration and cancer. Nat. Chem. Biol 5, 100–107 (2009). [PubMed: 19125156]
37. Tchoukalova YD, Votruba SB, Tchkonia T, Giorgadze N, Kirkland JL, Jensen MD, Regional differences in cellular mechanisms of adipose tissue gain with overfeeding. Proc. Natl. Acad. Sci. U.S.A 107, 18226–18231 (2010). [PubMed: 20921416]
38. Masuzaki H, Paterson J, Shinyama H, Morton NM, Mullins JJ, Seckl JR, Flier JS, A transgenic model of visceral obesity and the metabolic syndrome. Science 294, 2166–2170 (2001). [PubMed: 11739957]
39. Wabitsch M, Brenner RE, Melzner I, Braun M, Möller P, Heinze E, Debatin K-M, Hauner H, Characterization of a human preadipocyte cell strain with high capacity for adipose differentiation. Int. J. Obes. Relat. Metab. Disord 25, 8–15 (2001). [PubMed: 11244452]
40. Rutkowski JM, Stern JH, Scherer PE, The cell biology of fat expansion. J. Cell Biol 208, 501–512 (2015). [PubMed: 25733711]
41. Morrison RF, Farmer SR, Hormonal signaling and transcriptional control of adipocyte differentiation. J. Nutr 130, 3116S–3121S (2000). [PubMed: 11110883]
42. Roberto CA, Swinburn B, Hawkes C, Huang TT-K, Costa SA, Ashe M, Zwicker L, Cawley JH, Brownell KD, Patchy progress on obesity prevention: Emerging examples, entrenched barriers, and new thinking. Lancet 385, 2400–2409 (2015). [PubMed: 25703111]
43. McLaughlin T, Sherman A, Tsao P, Gonzalez O, Yee G, Lamendola C, Reaven GM, Cushman SW, Enhanced proportion of small adipose cells in insulin-resistant vs insulin-sensitive obese individuals implicates impaired adipogenesis. Diabetologia 50, 1707–1715 (2007). [PubMed: 17549449]
44. Muise ES, Azzolina B, Kuo DW, El-Sherbeini M, Tan Y, Yuan X, Mu J, Thompson JR, Berger JP, Wong KK, Adipose fibroblast growth factor 21 is up-regulated by peroxisome proliferator-activated receptor γ and altered metabolic states. Mol. Pharmacol 74, 403–412 (2008). [PubMed: 18467542]
45. Jonker JW, Suh JM, Atkins AR, Ahmadian M, Li P, Whyte J, He M, Juguilon H, Yin Y-Q, Phillips CT, Yu RT, Olefsky JM, Henry RR, Downes M, Evans RM, A PPARγ–FGF1 axis is required for adaptive adipose remodelling and metabolic homeostasis. Nature 485, 391–394 (2012). [PubMed: 22522926]
46. Zhang HH, Kumar S, Barnett AH, Eggo MC, Ceiling culture of mature human adipocytes: Use in studies of adipocyte functions. J. Endocrinol 164, 119–128 (2000). [PubMed: 10657847]

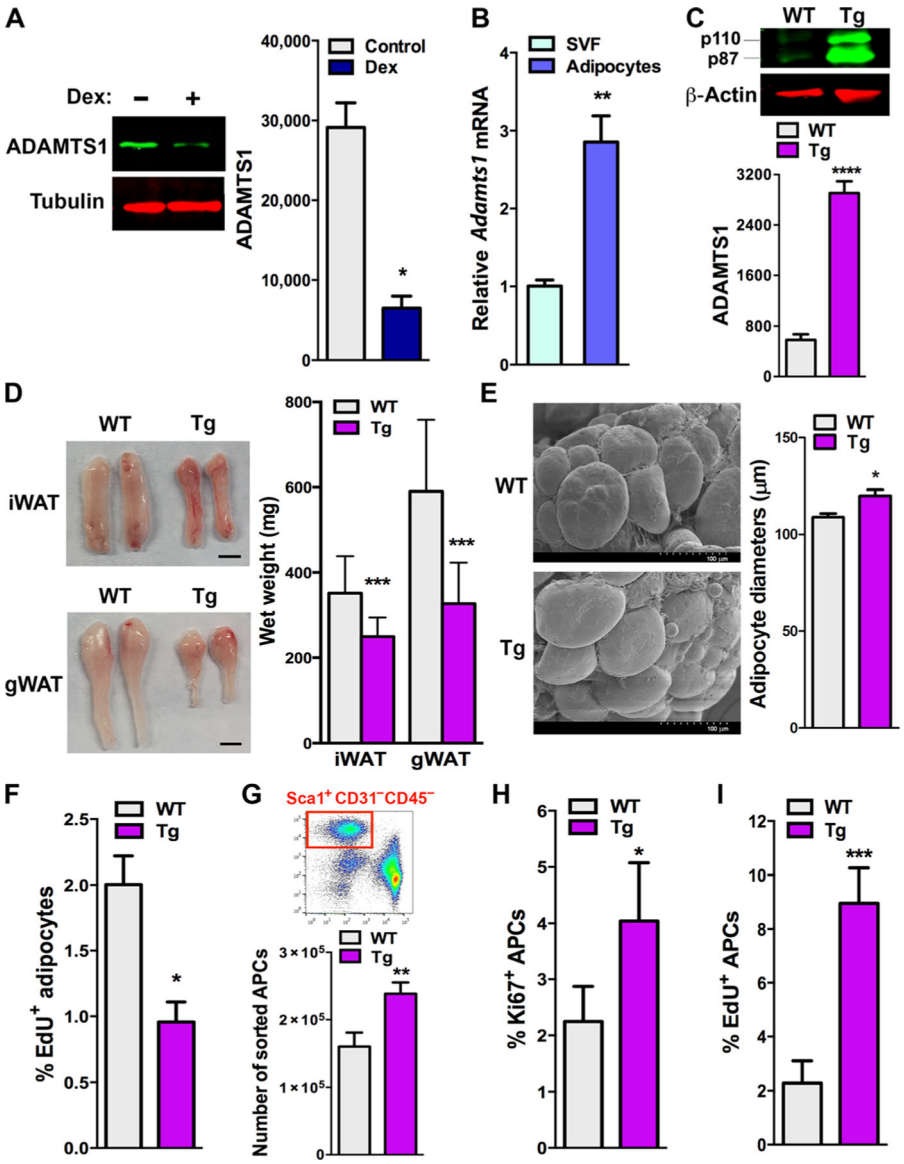

Fig. 1. ADAMTS1 in adipose tissue is responsive to systemic glucocorticoids.

(**A**) Immunoblots of adipose tissue harvested from male wild-type (WT) mice after the administration of systemic glucocorticoids [dexamethasone (Dex)] or ethanol control (left). Quantification of immunoblots shows a reduction in ADAMTS1 abundance in adipose tissues after systemic treatment with dexamethasone (n = 3 mice for each treatment) (right). (**B**) RT-qPCR of endogenous *Adamts1* expression in SVF cells compared to mature adipocytes (n = 3 independent experiments). (**C**) Immunoblots of adipose tissue from *Adam Tg* (Tg) mice probed with anti-ADAMTS1 antibody demonstrate overexpression of ADAMTS1 compared to gender-matched WT littermate (top). Quantification of immunoblots shows significant amounts of overexpressed ADAMTS1 in *Adam Tg* compared to WT adipose tissue (n = 3 mice for each genotype) (bottom). (**D**) Images (left) and quantification (right) of wet weights of inguinal (iWAT) and perigonadal (gWAT) white adipose tissue depots of 5-week-old male *Adam Tg* mice compared to WT littermate

controls (n = 8 mice for each genotype). Scale bars, 5 mm. (**E**) Scanning electron micrographs (left) and quantification (right) of average diameters of adipocytes in iWAT from male *Adam Tg* and WT mice (n = 3 mice for each genotype). (**F**) Fluorescence-activated cell sorting (FACS) analysis of mature adipocytes isolated from entire iWAT depots from *Adam Tg* compared to WT littermate mice (n = 3 mice for each genotype). (**G**) FACS plot (top) indicating the gating for FACS of iWAT SVF to isolate APCs. Quantification (bottom) of APCs in entire iWAT depots in *Adam Tg* compared to WT littermates (n = 6 mice for each genotype). (**H** and **I**) FACS of APCs isolated from iWAT of *Adam Tg* mice compared to WT littermates quantifying the fold increase in Ki67-positive ($Ki67^+$) and EdU^+ APCs in *Adam Tg* mice (n = 7 mice for each genotype). Additional examples of FACS plots and unstained negative control plots can be found in fig. S2A. $*P < 0.05$, $**P < 0.01$, $***P < 0.001$. P values were calculated by t tests. Error bars represent SDs.

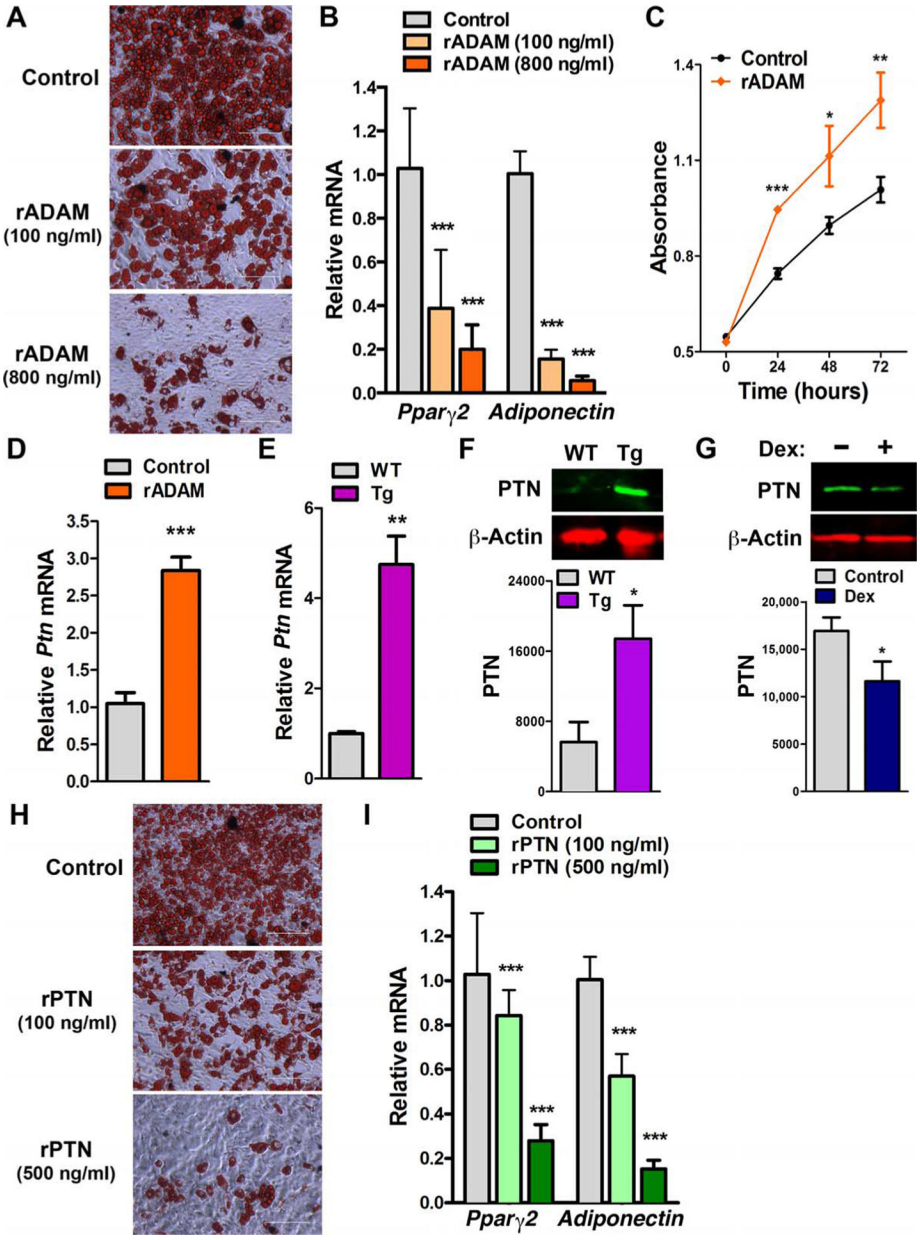

Fig. 2. Adipocyte-secreted ADAMTS1 drives APCs to proliferate rather than differentiate.

(**A**) Light-phase microscopy of APCs 8 days after induction of differentiation and stained with Oil Red O. The addition of rADAM to the culture medium blocks the appearance of lipid-laden mature adipocytes compared to APCs cultured with BSA (control). Scale bars, 100 μm. Images are representative of five sets of APCs for each treatment. (**B**) RT-qPCR of the expression of genes encoding markers of adipogenesis quantifying the effect of rADAM on adipocyte differentiation ($n = 5$ independent experiments). (**C**) XTT [2,3-bis(2-methoxy-4-nitro-5-sulfophenyl)-2*H*-tetrazolium-5-carboxanilide] assays to compare the rate of proliferation of rADAM-treated APCs with BSA (control)–treated APCs ($n = 3$ independent experiments). (**D**) RT-qPCR of WT APCs treated with rADAM quantifying the induction of *Ptn* expression compared to APCs treated with BSA (control) ($n = 3$

independent experiments). (**E**) RT-qPCR quantifying the increase in *Ptn* expression in the WAT of *Adam Tg* mice compared to WT littermate controls ($n = 3$ independent experiments). (**F**) Immunoblots (top) with quantification (bottom) of PTN in adipose tissue showing increased PTN abundance in *Adam Tg* mice ($n = 3$ independent experiments). (**G**) Immunoblots (top) with quantification (bottom) of PTN in adipose tissue harvested from dexamethasone-treated WT mice ($n = 3$ independent experiments). (**H**) Light microscopy (images are representative of three sets of APCs for each treatment) and (**I**) RT-qPCR ($n = 3$ independent experiments) of adipogenesis markers of WT APCs treated with rPTN or BSA (control) 8 days after induction of adipogenesis and stained with Oil Red O. Scale bars, 100 μm. $*P < 0.05$, $**P < 0.01$, $***P < 0.001$. *P* values were calculated by *t* tests. Error bars represent SDs.

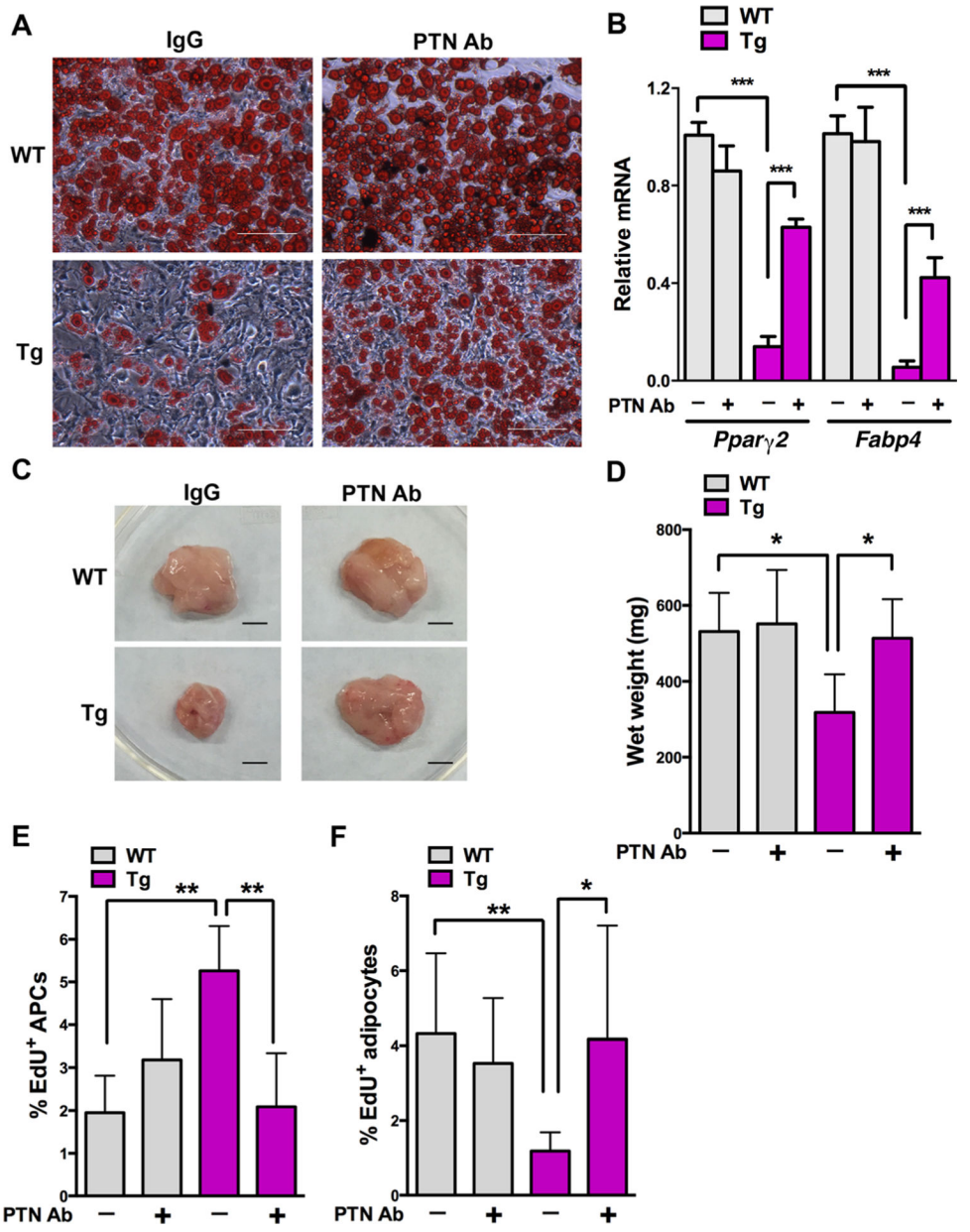

Fig. 3. PTN is essential for the effect of ADAMTS1 on APCs.

(**A**) Light-phase microscopy of APCs from WT and *Adam Tg* mice 8 days after induction of adipogenesis and treatment with PTN neutralizing antibody (PTN Ab) or IgG control antibody (IgG) and stained with Oil Red O. Neutralizing PTN rescues the *Adam Tg* APCs from the block in differentiation. Scale bars, 100 μm. Images are representative of five sets of APCs for each treatment. (**B**) RT-qPCR of adipocyte differentiation markers in *Adam Tg* APCs treated with PTN neutralizing antibody quantifying the extent of rescue from the block in differentiation compared to IgG control–treated APCs ($n = 5$ independent experiments). (**C** and **D**) Images and quantification of iWAT mass from mice after in vivo treatment with PTN neutralizing antibody or IgG control ($n = 6$ mice for each treatment and genotype). Scale bars, 5 mm. (**E**) FACS of EdU^+ APCs in WT and *Adam Tg* iWAT after in

vivo PTN neutralizing antibody or control IgG treatment shows that neutralizing PTN in *Adam Tg* mice restores APC proliferation to WT values ($n = 8$ mice for each treatment and genotype). (**F**) FACS of EdU^+ adipocytes in WT and *Adam Tg* iWAT after in vivo PTN neutralizing antibody (+) or control IgG (−) treatment shows that neutralizing PTN in *Adam Tg* mice restores adipogenesis to WT values ($n = 8$ mice for each treatment and genotype). $^*P < 0.05$, $^{**}P < 0.01$, $^{***}P < 0.001$. *P* values were calculated by *t* tests. Error bars represent SDs.

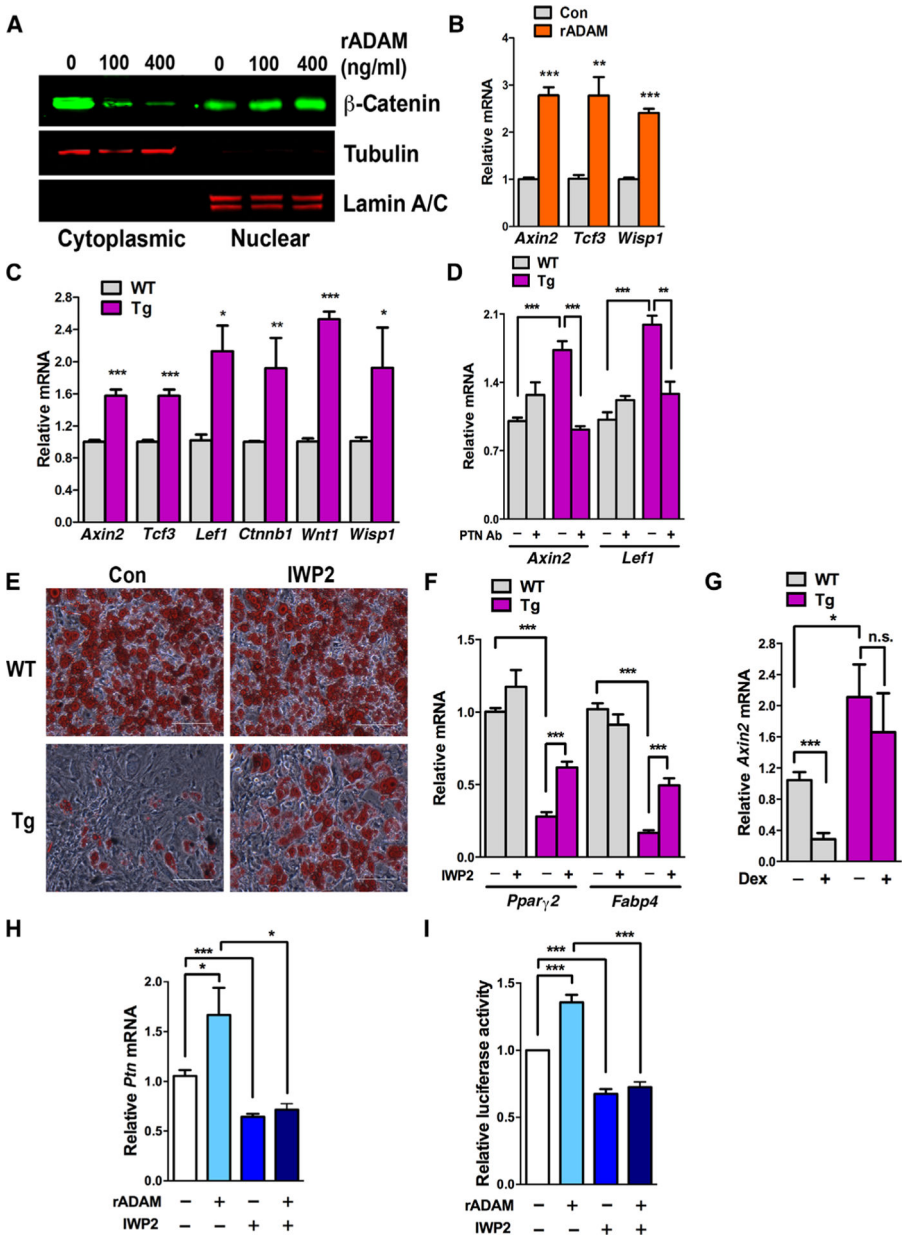

Fig. 4. Glucocorticoids intersect with Wnt signaling through ADAMTS1.

(**A**) Immunoblots of nuclear and cytoplasmic fractions of APCs harvested from WT animals and exposed to a titration of rADAM. Tubulin and Lamin A/C confirm segregation of cytoplasmic and nuclear fractions, respectively. $n = 3$ independent experiments. (**B**) RT-qPCR quantifying the expression of TCF/LEF target genes in APCs exposed to rADAM ($n = 3$ independent experiments). (**C**) RT-qPCR on APCs directly isolated from *Adam Tg* mice or WT littermate controls quantifying TCF/LEF target gene activation ($n = 5$ independent experiments). (**D**) RT-qPCR quantifying *Axin2* and *Lef1* expression in APCs harvested from *Adam Tg* and WT mice after PTN neutralizing antibody (+) or IgG control (−) treatment ($n = 3$ independent experiments). (**E**) Light-phase microscopy of APCs isolated from *Adam Tg* or WT mice 8 days after induction of adipocyte differentiation with cotreatment with the

Wnt inhibitor IWP2 or dimethyl sulfoxide vehicle control (Con) and stained with Oil Red O. Scale bars, 100 μm. Images are representative of three sets of APCs for each treatment. (**F**) RT-qPCR of adipocyte differentiation markers quantifying the rescue of adipocyte differentiation in APCs from *Adam Tg* mice treated with IWP2 ($n = 3$ independent experiments). (**G**) RT-qPCR of *Axin2* expression in primary APCs isolated from *Adam Tg* and WT mice treated with dexamethasone (+) or ethanol control (−) quantifying the effect of systemic glucocorticoids on Wnt signaling in APCs and the ability of Adamts1 to block this signal ($n = 3$ independent experiments). (**H**) RT-qPCR quantifying *Ptn* expression in APCs isolated from WT mice and treated with rADAM, IWP2, or both ($n = 7$ independent experiments). (**I**) Relative luciferase reporter activity in cells transfected with a luciferase reporter construct containing the *Ptn* promoter and −1-kb promoter-proximal region ($n =$ 4independent experiments). $*P < 0.05$, $**P < 0.01$, $***P < 0.001$. n.s., not significant. *P* values were calculated by *t* tests. Error bars represent SDs.

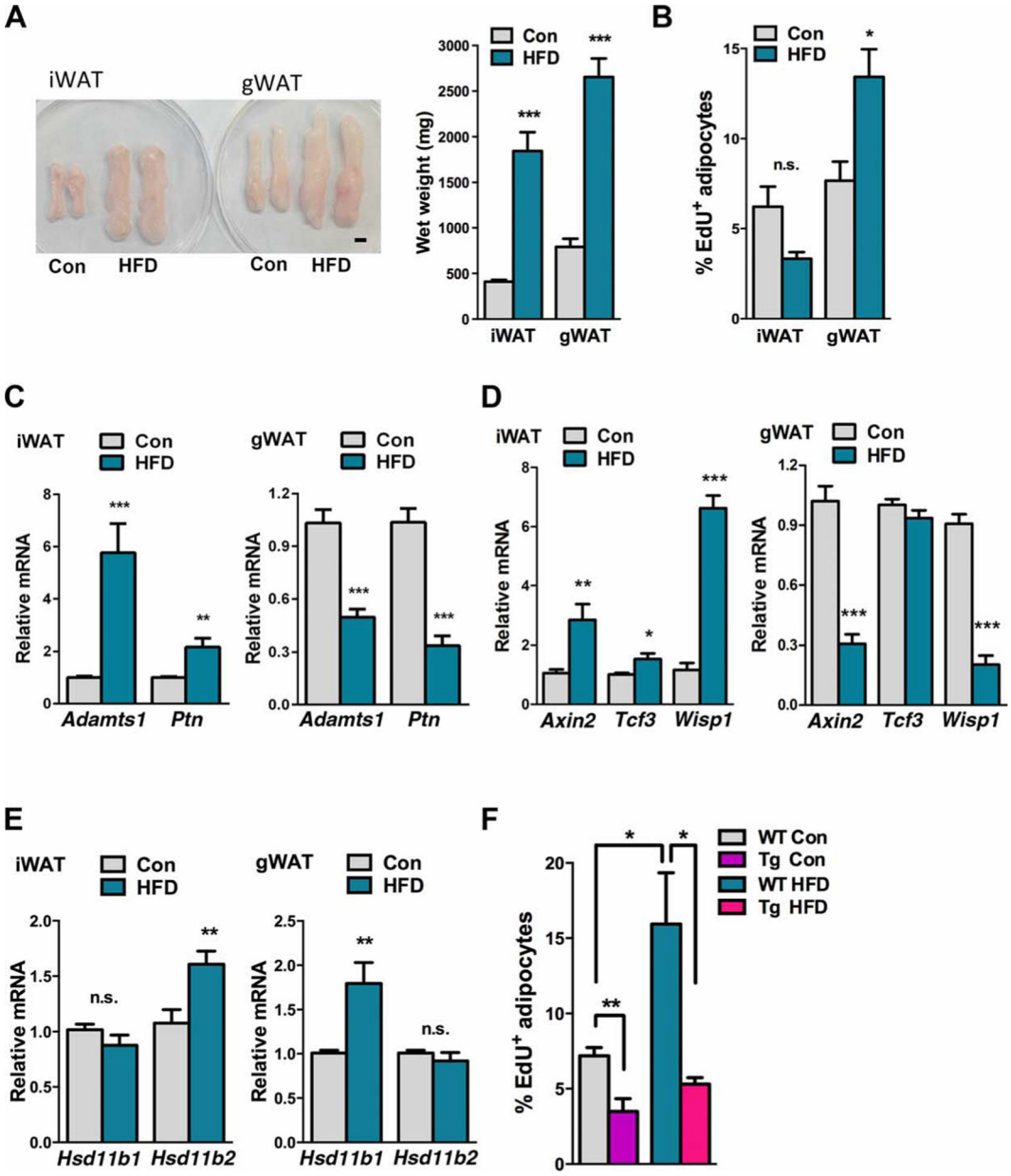

Fig. 5. HFD induces adipose depot–specific changes in *11bhsd* expression and the ADAMTS1-Wnt pathway.

(**A**) Images (left) and quantification (right) of the weights of iWAT and gWAT fat depots harvested from WT C57BL/6 mice after 3 months of HFD compared to WT mice on a standard chow diet (Con) (*n* = 8 mice for each treatment). Scale bar, 5 mm. (**B**) FACS analysis quantifying adipogenesis during an EdU pulse in WT mice fed HFD or standard diet (*n* = 8 mice for each diet). (**C**) RT-qPCR quantifying *Adamts1* and *Ptn* expression in iWAT (left) and gWAT (right) adipose tissue depots harvested from WT mice fed an HFD or a standard chow diet (*n* = 8 mice for each diet). (**D**) RT-qPCR quantifying the expression of TCF/LEF target genes in iWAT (left) and gWAT (right) adipose tissue depots harvested from WT mice fed an HFD or a standard chow diet (*n* = 3 independent experiments). (**E**) RT-qPCR quantifying the expression of *11bhsd1* and *11bhsd2* in iWAT (left) and gWAT (right)

adipose tissue depots harvested from WT mice fed an HFD or a standard chow diet ($n = 3$ independent experiments). (**F**) FACS analysis quantifying adipogenesis during an EdU pulse in *Adam Tg* mice compared to WT littermates fed a standard chow diet (WT, $n = 10$; *Adam Tg*, $n = 5$,) or HFD (WT, $n = 8$; *Adam Tg*, $n = 3$). $^{*}P < 0.05$, $^{**}P < 0.01$, $^{***}P < 0.001$. *P* values were calculated by *t* tests when two parameters were compared, and Bonferroni multiple comparison test was used when more than two parameters were compared. Error bars represent SDs.

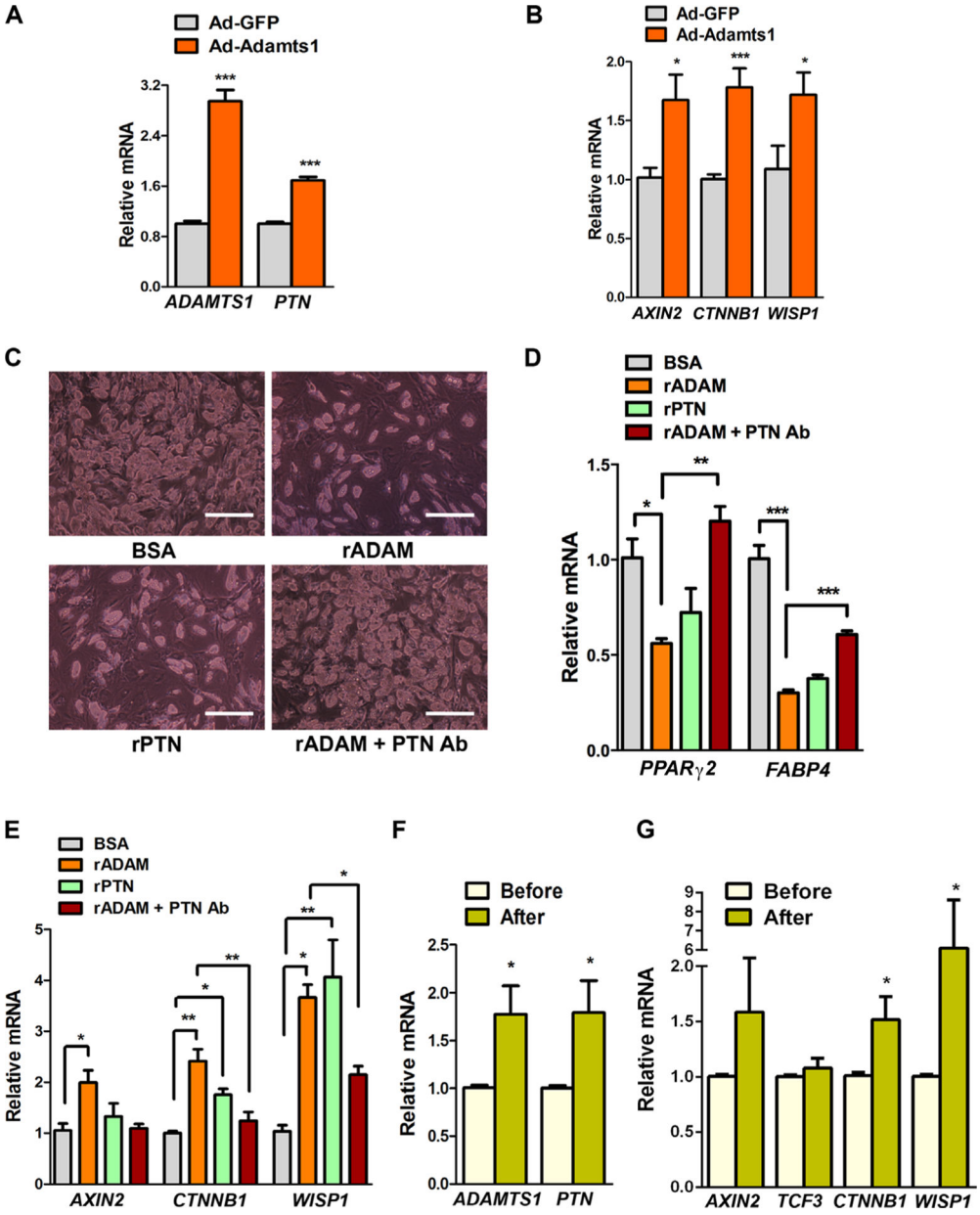

Fig. 6. The Adamts1 pathway is conserved in humans.

(**A**) RT-qPCR quantifying *ADAMTS1* and *PTN* expression in primary human SVF infected with Adamts1-adenovirus (Ad-Adamts1) compared to green fluorescent protein (GFP)–adenovirus–infected cells (Ad-GFP) ($n = 3$ independent experiments). (**B**) RT-qPCR quantifying the expression of TCF/LEF target genes in primary human SVF infected with Ad-Adamts1 compared to Ad-GFP ($n = 3$ independent experiments). (**C**) Light-phase microscopy of human SVF 8 days after induction of adipogenesis. Treatment with rADAM or rPTN with the induction of differentiation blocks adipocyte differentiation. PTN neutralizing antibody rescues the human cells from the block in differentiation. Scale bars, 200 μm. Images are representative of three sets of SVF for each treatment. (**D**) RT-qPCR of markers of adipocyte differentiation quantifying the block in differentiation caused by

rADAM and rPTN as well as the rescue of the rADAM block in adipocyte differentiation with PTN neutralizing antibody ($n = 3$ independent experiments). (**E**) RT-qPCR of human SVF quantifying the induction of TCF/LEF target genes when cells are treated with human rADAM and rPTN, and the block in induction when cells are cotreated with PTN neutralizing antibody ($n = 3$ independent experiments). (**F**) RT-qPCR quantifying the expression of *ADAMTS1* and *PTN* in SVF from subcutaneous adipose tissue biopsies obtained from human volunteers before and after eating a high-calorie diet for 4 weeks ($n = 6$). (**G**) RT-qPCR quantifying the expression of TCF/LEF target genes in SVF from subcutaneous adipose tissue biopsies obtained from human volunteers before and after eating a high-calorie diet ($n = 6$). $^{*}P < 0.05$, $^{**}P < 0.01$, $^{***}P < 0.001$. *P* values were calculated by *t* tests when two parameters were compared, and Bonferroni multiple comparison test was used when more than two parameters were compared. Error bars represent SDs.